The University of Tehran Press

Pollution

Print ISSN: 2383-451X
Online ISSN: 2383-4501

https://jpoll.ut.ac.ir/

Improving CO_2 Capture Performance of Aqueous MDEA Through Hybridization of Sulfolane and MIL-101-NH_2(Cr)

Razieh AghehroChaboki[1] | Alireza Asghari[1]✉ | Ahmad Tavasoli[2] | Maryam Rajabi[1]

1. Department of Chemistry, Semnan University, Semnan, Iran
2. School of Chemistry, College of Science, University of Tehran, Tehran, Iran

Article Info

Article type:
Research Article

Article history:
Received: 9 September 2025
Revised: 22 November 2025
Accepted: 06 February 2026

Keywords:
CO_2 absorption
Regeneration efficiency
High-pressure absorption
Hybrid solvent
Metal Organic Framework (MOF)

ABSTRACT

To improve the absorption and desorption performance of aqueous MDEA solution, a hybrid solvent composed of 40 wt.% MDEA and 20 wt.% Sulfolane was prepared and systematically evaluated under varying pressure conditions. At (0.1–0.5 MPa) pressures, the conventional aqueous MDEA solution exhibited a higher CO_2 absorption capacity in comparison to the hybrid solution, indicating its effectiveness in less pressurized environments. However, under high-pressure (>0.5 MPa) conditions, the hybrid solution demonstrated superior performance, reaching 3.28 mol·kg^{-1} CO_2 molality, compared to 2.94 mol·kg^{-1} for the conventional solution. This enhanced capacity highlights the beneficial interaction between MDEA and sulfolane at elevated pressures. Additionally, the hybrid formulation improved the regeneration efficiency by 3.7% relative to the standard MDEA solution, indicating better solvent recyclability. The incorporation of 0.1 wt.% MIL-101-NH_2(Cr) nanoparticles into the hybrid solvent further enhanced system performance, increasing CO_2 molality by 17.1% suggesting enhanced surface area, the porous surface, the amine functional groups and active site availability for CO_2 interaction. elevating the regeneration efficiency to 99.45% at an operating temperature of 80°C, demonstrating the underscoring the synergistic role of nanomaterials in advancing solvent-based CO_2 capture technologies.

Cite this article: AghehroChaboki, R., Asghari, A., Tavasoli, A., & Rajabi, M. (2026). Improving CO_2 Capture Performance of Aqueous MDEA Through Hybridization of Sulfolane and MIL-101-NH_2(Cr). *Pollution*, 12(1), 433-447. https://doi.org/10.22059/poll.2025.402056.3109

 Publisher: The University of Tehran Press.
DOI: https://doi.org/10.22059/poll.2025.402056.3109

INTRODUCTION

CO_2 is the primary greenhouse gas contributing to global warming which may reach 550 ppm by 2050. Natural gas is a major energy source for power generation facilities and residential applications. However, its combustion releases CO_2 into the atmosphere. Notably, natural gas combustion emits fewer particulates than other fossil fuels. Therefore, the reduction of CO_2 emissions and their elimination has been the focus of various researchers around the world (Gouedard et al., 2012; Liang et al., 2016).

Various methods such as membrane processes, absorption, and solid adsorbents (zeolites, silica, Metal Organic Frameworks (MOF)) have been explored for CO_2 separation (Gouedard et al., 2012; Piscopo & Loebbecke, 2020). The removal of carbon dioxide from process gas streams is an important step in many industrial processes. If CO_2 is not sufficiently extracted from natural gas, it can cause corrosion, reduce the gas's calorific value (and consequently

*Corresponding Author Email: *aasghari@semnan.ac.ir*

its market price), and have detrimental environmental effects. Solvent-based absorption techniques are among the most widely recognized and effective approaches for CO_2 removal (Borhani et al., 2018). Over the years, alkanolamines have emerged as the best-known solvents used for CO_2 absorption. However, it still presents several challenges, including difficulties in reclaiming contaminants, unsuitability for treating gas streams with high CO_2 concentrations, and the formation of corrosive degradation products in the presence of CO_2.

MDEA is frequently employed in amine-based gas treating plants due to several advantages: it does not form stable carbamates, exhibits a lower corrosion rate compared with other alkanolamines, can be used in aqueous solutions at concentrations up to 60 wt.% without significant solvent losses, and demonstrates high resistance to degradation. Nevertheless, MDEA also has drawbacks, including a lower heat of reaction and a slower reaction kinetics with CO_2, as well as the tendency for water to migrate into the gas stream during the absorption process (Borhani et al., 2018). In physical absorption processes, gas absorption takes place under high-pressure conditions. In addition, the pressure can be lowered to regenerate the solvent. Heat is not needed like it is for chemical absorption (Kidnay et al., 2019). MOFs are a novel class of materials formed by the integration of organic ligands and metal centers. In contrast to traditional adsorbents, their distinctive characteristics, including facile synthesis, extensive surface area, tunable pore dimensions, and the presence of metal active sites, demonstrate significant potential for CO_2 and H_2S removal applications (Belmabkhout et al., 2016).

Numerous researches have been done in the field of CO_2 and H_2S removal using nanofluids. Irani et al. (2018) used functionalized poly-ethylene-imine (PEI) to improve CO_2 absorption and showed that addition of 0.1 wt.% GO to the amine solution increases absorption capacity by 9.6%. Zheng et al. (2013) studied CO_2 absorption with 2-amino-2-methyl-1-propanol (AMP) in the presence of TEG and DEG physical solvents. The solubility of CO_2 in the presence of DEG was higher than TEG. Ghasemi et al (2020) studied the addition of ZIF-90 to MDEA/GO nanofluid. The amount of carbon dioxide absorption increased by 23%. They investigated the effect of partial pressure and temperature on the absorption capacity and the results indicated that the temperature had a negative effect on the performance of the system (Ghasemi et al., 2020). Moreover, Nozaeim et al. (2022) investigated CO_2 absorption using DEEA aqueous solution and DEEA-sulfolane mixed solution. They observed that replacing water with sulfolane in DEEA solution increases the absorption rate as well as the cyclic capacity.

The aim of this study was to evaluate CO_2 absorption and regeneration performance of aqueous MDEA and MDEA–sulfolane hybrid solvents under various operating conditions. This laboratory-scale assessment provides data for selecting suitable solvents for CO_2 capture and gas sweetening applications. In addition, metal–organic framework (MOF) materials were incorporated to enhance CO_2 absorption. Although MOFs have shown promise in CO_2 capture, their integration into hybrid solvent systems has been investigated only in a limited number of studies. In this work, a MIL-101-NH_2(Cr)-based nanostructured material with enhanced CO_2 absorption capacity was synthesized and dispersed in amine solvents, with the potential to reduce the required amine concentration in gas sweetening processes.

MATERIALS AND METHODS

Materials

The materials used in this study were employed without additional purification. The absorbents used in the experiments were supplied by Merck and Sigma-Aldrich. gases were supplied by domestic manufacturers and had purities of 99.5%.

Synthesis and preparation of nanoparticles

The hydrothermal technique was employed for nanoparticle synthesis. To prepare the MIL-

101-NH_2(Cr), 800 mg (2 mmol) of $Cr(NO_3)_3 \cdot 9H_2O$, 360 mg (2 mmol) of 2-aminoterephthalic acid, and 200 mg (5 mmol) of NaOH were each dissolved in 15 ml of deionized water. The resultant solutions were mixed and stirred for 30 minutes at ambient temperature. The mixture was transferred to a 50 mL stainless steel autoclave, heated at 150°C for 12 hours and subsequently allowed to cool to room temperature naturally. A green precipitate was produced after the reaction. The precipitate was obtained using centrifugation, washed twice with DMF, and subsequently activated in an autoclave at 100 °C for 12 hours with ethanol as the solvent. The obtained solid was dried in a vacuum oven at a temperature of 80 °C for 12 hours (Xu et al., 2021).

Preparation of suspension

To prepare the nanofluid (0.1% by weight), the nanostructure was poured into a 100 ml flask. Then 40 wt.% methyldiethanolamine (MDEA), 20 wt.% sulfolane and 39.9wt.% deionized water was added to the mixture. Then, the mixture was then placed in an ultrasonic bath at room temperature for 20 minutes.

Characterization

The stability of the nanofluid was assessed using zeta potential analyzer from Malvern Instruments Ltd. The physical and chemical properties of MIL-101-NH_2(Cr) were analyzed to identify the functional groups, crystal structure, porous architecture, and surface morphology using various techniques. These techniques include Brunauer-Emmet-Teller (BET; BELSORP Mini IL Japan), X-ray diffraction (XRD; Bruker, D8 ADVANCE), Fourier transform infrared spectroscopy (FT-IR; Bruker, ISS-88), scanning electron microscope (USA, FEL; Quantum 2000, SEM), transmission electron microscope (TEM; EM208, Philips), and thermal gravimetric analysis (Perkin-Elmer, USA).

Apparatus and procedure

Details of the experimental method to measure gas absorption have been reported in our previous studies (Zheng et al., 2013). Figure 1 shows the reactor system. First, a scale with a 0.0001 accuracy is used to measure the exact amount of freshly prepared solutions (Aqueous MDEA, Hybrid solution and Hybrid solution + MOF nanoparticles) were injected to the reactor, with a volume of $V_{cell} \approx 131.8 \pm 1.0$ cm³. The cell temperature was controlled using a water circulation bath (T 2500 PMT Tamson) that was attached to a double-walled reactor. A Pt-100 sensor and a digital thermometer (TM-917 utron) with a resolution of 0.01 K was positioned in the cell. Pressure transmitters (KELLER) which can be adjusted from zero to twenty-five, were placed in the equilibrium cell. The temperature of the bath was varied from 313.15 to 353.15 K. The capsule was filled with carbon dioxide. After the CO_2 injection to the cell, and once it reached equilibrium, its pressure and temperature carefully recorded. To obtain the amount of CO_2 injected into the balance cell, the following equation was used (Bahadori et al., 2024):

$$n_{total} = \left(\rho_i - \rho_f\right).V_{gc} = n_i - n_f \quad (1)$$

Where V_{gc}, ρ_i, ρ_f respectively are the volumes of the gas container, initial and final molar density of CO_2 at gas container just before and after the gas injection. The amount of CO_2 in the liquid phase in each injection n_{co2}^{l} can be determined by:

$$n_{co2}^{l} = n_{total} - n_{co2}^{g} \quad (2)$$

where n_{total} and n_{co2}^{g} respectively are the total number of CO_2 moles cumulatively injected into the cell and the number of moles of CO_2 in the gas phase obtained by Eq. (3).

$$n_{co2}^{g} = \rho_{co2}^{g}.V_{g} \tag{3}$$

where Vg is the gas-phase volume obtained by Eq. (4), ρ_{co2}^{g} is the molar density of CO_2 in the gas phase at P_{CO2} and test temperature (T = 313.15-353.15 K) obtained from National Institute of Standards and Technology (NIST).

$$V_{g} = 0.1318/dm^{3} - V_{unloaded\ solvent} \tag{4}$$

where $V_{unloaded\ solvent}$ is the volume of the unloaded solvent at interest temperature (T = 313.15 -353.15 K) estimated by density of aqueous MDEA solution. The density H_2O/MDEA/SFL solution was measured in the laboratory with a pycnometer (density at T = 313.15 K equals to 1.07332 g. cm^{-3}).

Finally, using Eqs. (1)-(4), CO_2 absorption on loading, α_{CO_2}, and molality, M_{CO_2}, respectively were obtained by Eqs. (5)-(6):

$$\alpha_{CO_2} = \frac{n_{CO_2}^{l}(mol)}{n_{\mathrm{MDEA}}} \tag{5}$$

$$M_{CO_2} = \frac{n_{CO_2}^{l}(mol)}{w_{unloaded\ solvent}} \tag{6}$$

In which, $n_{CO_2}^{l}$, n_{MDEA} are the amount of CO_2 and MDEA in the liquid phase, respectively and $w_{unloaded\ solvent}$ is mass of fresh nanofluid solvent (gas-unloaded) in kg.

The uncertainty of CO_2 solubility can be calculated:

$$\frac{u(\alpha)}{\alpha} = \pm\sqrt{\left[\frac{u\left(n_{CO_2}^{'}\right)}{n_{CO_2}^{'}}\right] + \left[\frac{u(n_{\mathrm{MDEA}})}{n_{\mathrm{MDEA}}}\right]} = \sqrt{\frac{u(n_i)^2 + u(n_f)^2 + u\left(n_{CO2}^{g}\right)^2}{\left(n_{CO2}^{'}\right)^2} + \frac{u(n_{MDEA})^2}{(n_{MDEA})^2}}$$

where $u(n_f)$, $u(n_i)$ and u $(n_{CO_2}^{'})$ are calculated by the following equation:

$$\frac{u(n_k)}{n_k} = \pm\sqrt{\left(\frac{u(p_k)}{p_k}\right)^2 + \left(\frac{u(V_k)}{V_k}\right)^2 + \left(\frac{u(T_k)}{T_k}\right)^2}$$

u (n_{MDEA}) is taken from the purity of MDEA reported by the supplier.

The uncertainty of the pressure sensors and $u(p_k)$=± 0.0003 MPa and u (T_K)=± 0.10 K and these values are the same for the volume of the gas sample and the equilibrium cell and are equal to $u(V_k) = \pm 1 cm^3$ (Bahadori et al., 2024). Before starting with the prepared solutions, the accuracy of the system was evaluated. For this purpose, the absorption curves with the 40 wt.% MDEA aqueous solutions that are present in the reported sources are reproduced by this system, and the results are compared (Bahadori et al., 2024).

RESULTS AND DISCUSSION

Validation test

This approach and its setup were validated by multiple CO_2 experiments to ensure accuracy. The solubility results were compared to what was already published in the literature. The validation tests were conducted at a temperature of 313.15 K using methyl diethanolamine

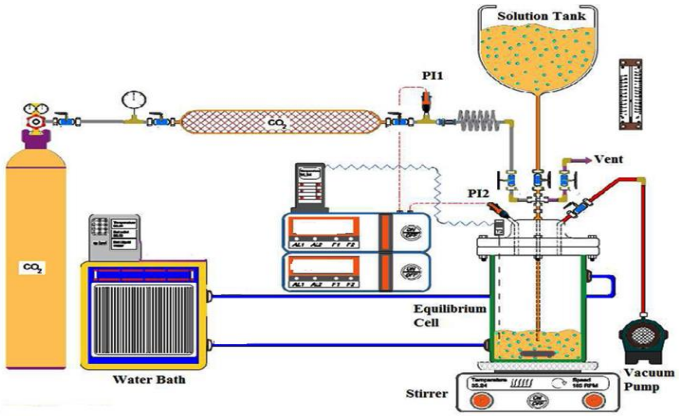

Fig. 1. Schematic diagram of CO_2 solubility measurement.

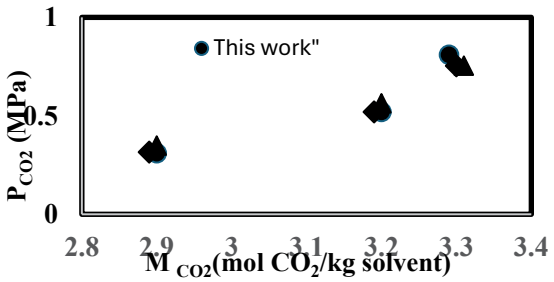

Fig.2 (on the left) Validation experiments for solubility of CO_2 in 40 wt.% MDEA at 313.15 k.

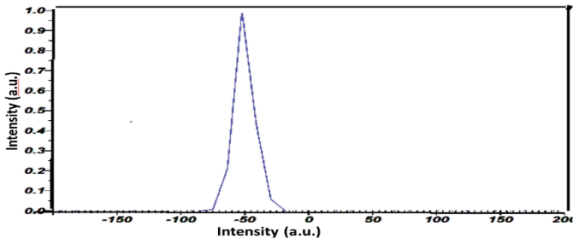

Fig.3. (on the right) Zeta potential for a solution of 40% MDEA, 20% sulfolane, and 0.1% by weight of MIL-101-NH_2 (Cr)

(MDEA) aqueous solutions that were 40% by weight. Our findings are consistent with the other data presented, as seen in Figure 2 (Maleki et al., 2018; Vahidi, 2016).

Zeta potential

A common method for assessing nanofluid stability is photographing the sediment. In this method, after the suspension is prepared, it is photographed during different times, and the amount of precipitation is determined. Applying the zeta potential is an additional strategy. Suspension stability is enhanced by an increase in the electrostatic repulsion between particles, which occurs when the absolute value of the zeta potential is large. Particle aggregation is minimized when surface charge is sufficiently high surface charge. In general, stable suspensions are defined as those having an absolute zeta potential value greater than ±25mv (Ghadimi et al., 2011). Figure 3 demonstrates that the sample with 0.1% nanoparticles by weight in the base fluid had a zeta potential value of -50 mv, indicating that the suspension was stable.

FTIR spectroscopy

Infrared spectroscopy, IR is a method to identify molecules and especially the functional groups of molecules. For MIL-101-NH_2 (Cr) sample as can be seen in Figure 4, the observed peaks in the range of (400-800) cm^{-1} and 767 cm^{-1} are related to stretching vibrations of oxygen with metals and Cr-O vibrations. The peak in 1387 cm^{-1} is C-N stretching vibrations on the aromatic ring, the peak in 1429 cm^{-1} is C=O double bond in terephthalic, the peak in 1565 cm^{-1} is N-H bending vibrations, and a broad peak in the range of 3000 to 3500 cm^{-1} indicate the presence of free amines. The two index peaks at 3356 cm^{-1} which correspond to the symmetric vibrations of NH_2 and 3490 cm^{-1} confirm the stretching vibrations of O-H in the chromium center (Tian et al., 2016).

Thermogravimetric Analysis (TGA)

Figure 5 shows the thermogravimetric curve of MIL-101-NH_2(Cr). The initial weight loss at 80-130^oC temperatures is related to the loss of water molecules. 75% weight loss between 250 and 450^o C is related to the loss of solvents and the breakdown of the metal-organic frameworks. The thermal stability temperature of the sample was about 300 degrees Celsius. The maximum temperature for the regeneration of amine solution saturated with acid gases is about 130 degrees Celsius, and these results show that the nanostructure can be easily regenerated at such a temperature without decomposing the framework.

BET analysis

Using BET analysis Figure 6, the amount, size, and approximate shape of the pores of the MIL-101-NH_2(Cr) absorbent is obtained as specified in Table 1.

XRD pattern

XRD pattern of the nano particle is shown in Figure 7. The crystal structure of MIL-101-NH_2(Cr) are confirmed by the long and thin peaks observed at 9.1° and 19° angles, which are in

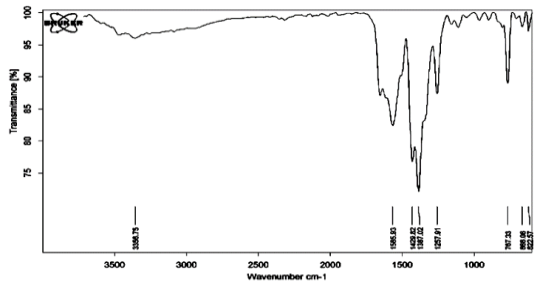

Fig.4. FTIR spectrum of MIL-101-NH_2 (Cr)

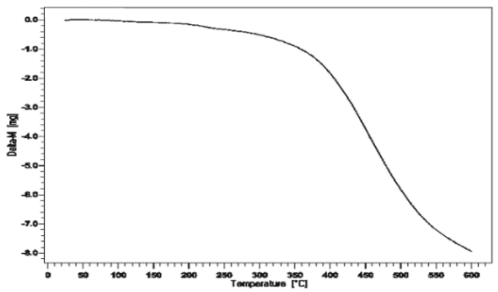

Fig. 5. The thermogravimetric curve of MIL-101-NH_2(Cr)

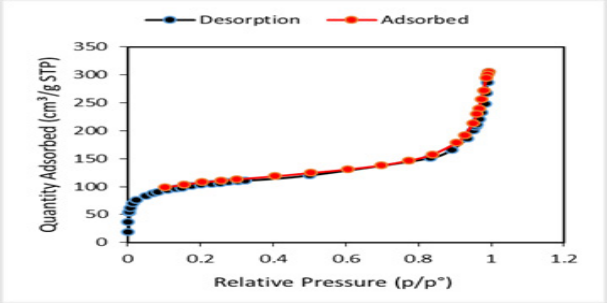

Fig. 6 (on the left) N_2 adsorption −desorption isotherms (77 K) MIL-101-NH_2(Cr)

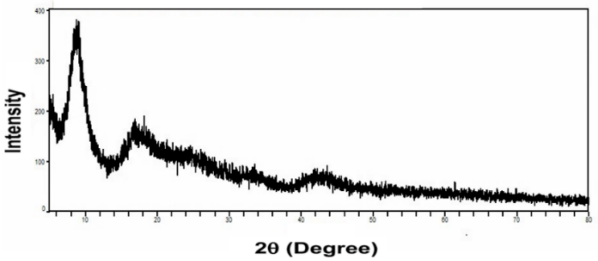

Fig.7. (on the right) XRD patterns of simulated MIL-101-NH_2(Cr)

Table 1. Textural Properties of Adsorbent

$S_{BET/m^2/g}$	$Pore\ volum^{BJH}$	Nanoparticle Size / nm Average:	Mean pore diameter/ nm	t-Plot $V\ /cm^3/g$ Micropore
339.5862	0.413402 cm^3/g	17.6686	3.64293	0.070238

agreement with all sources and references.

SEM and TEM images

SEM images of the MIL-101-NH_2 (Cr) are shown on Figure 8 (a, b). The figures reveal that the sample's almost crystalline morphology featured a relatively irregular and porous particle structure (Carretero-Cerdán et al., 2023). The transmission electron microscope (TEM) is used to image samples and analyze their surface characteristics and morphology. Figure 8 (c, d) also presents TEM images of the examined sample at two different magnifications. According to the figure, in the micrographs of this sample, particles with a quasi-spherical morphology can be seen. In order to check the particle size distribution in the investigated sample, several particles were measured from TEM images by Image J image processing software and the measured particle sizes were labeled on them. The statistical data related to these measurements are reported in the table 2.

Absorption tests

The absorption tests were performed at different temperatures and pressures. Initially, the absorption performance of a 40 wt.% aqueous MDEA solution was investigated at different temperatures and pressures. Next, the absorption of a hybrid solution containing 40 wt.% MDEA and 20 wt.% of the Sulfolane as a physical solvent is studied. Then, 0.1wt.% MIL-101-NH_2(Cr) nanostructure is added to the hybrid fluid (nano-fluid), and the absorption of nano-fluid was measured. Figure 9 (a-c) compares the molality of CO_2 for 40 wt.% aqueous MDEA and the MDEA+Sulfolane (40/20) hybrid solution in the temperature ranges of 40 to 80 °C, respectively. As shown in Figure 9, except at high pressures, the molality of CO_2 is higher

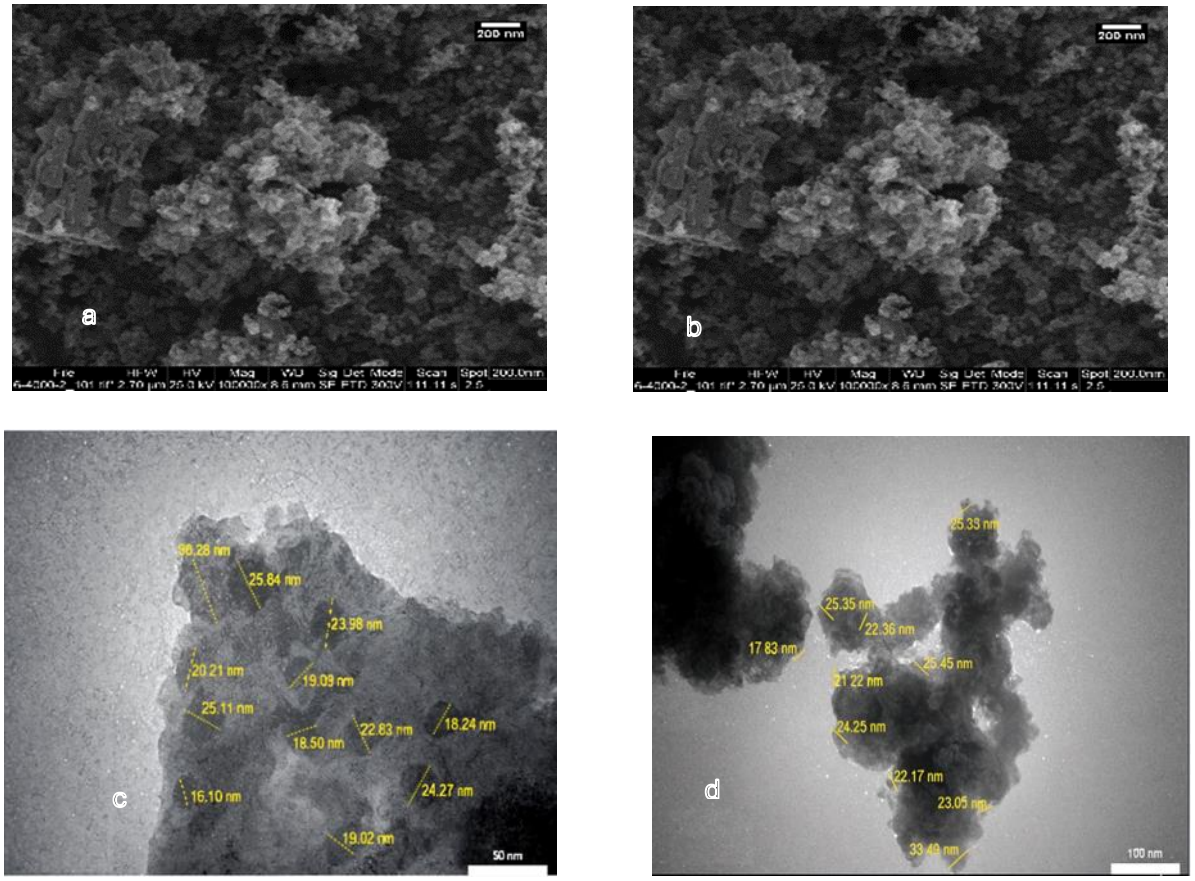

Fig. 8. SEM (a, b) and TEM (c, d), images of the MIL-101-NH_2 (Cr).

Table 2. Statistical results obtained in the samples studied

Total number of measurements	Average(nm)	Standard deviation(nm)	The smallest particle (nm)	Measured particle with average size(nm)	Largest particle (nm)
22	23.24	4.82	16.1	22.84	38.28

for 40 wt. % aqueous MDEA than that for hybrid solution. The decrease in the molality of CO_2 could be related to the decrease in the content of H_2O, which is essential for protonation of the alkanolamine. In addition, direct carbon-MDEA reactions occur in the presence of bicarbonate and water. The highest CO_2 absorption for MDEA aqueous solution occurred at the temperature of 313.15. At this temperature, the amount of absorption shows an increase of 12.67% compared to the hybrid solution. As mentioned, this reduction can be attributed to the decreased water content, which is essential for the protonation of the tertiary amine in MDEA (Luo et al., 2016). However, at elevated pressures, Sulfolane exerts its influence by enhancing CO_2 absorption through a physical mechanism. Physical solvent-based absorption processes rely on Henry's Law, which states that the solubility of a gas in a liquid increase with pressure. In such processes, solvent regeneration can typically be achieved by pressure reduction alone; unlike chemisorption, no external heat in put is required.

In aqueous solution, hydroxide and water react with CO_2 according to the following reactions:

$$CO_2 + 2H_2O \rightleftarrows H_3O^+ + HCO_3^- \quad (7)$$

$$CO_2 + OH^- \rightleftharpoons HCO_3^- \quad (8)$$

H_2O, CO_2 and MDEA react indirectly and produce protonated MDEA and bicarbonate. For this reaction, various mechanisms have been reported. MDEA accumulates with water before reacting with carbon dioxide, as schematically shown below.

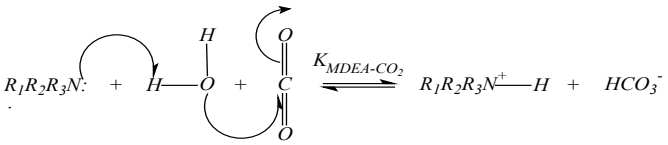

(9)

MDEA dissolves in water due to its hydroxyl (-OH) and amino groups, which increase its boiling point and lower its vapor pressure, thereby minimizing amine loss. Additionally, the presence of electron-donating groups and substituents attached to the nitrogen atom influences its absorption capacity.

For both cases, the molality of CO_2 decreased with increasing temperature (Figure 9). Absorption is an exothermic process, and as the temperature rises, gases become less soluble in liquids, reducing the absorption capacity (Yih & Sun, 1987). Regeneration efficiency which is the ratio of absorption capacity of the recovered solution to the absorption capacity of fresh solution, was also investigated for all cases. Figure 10 shows the regeneration efficiencies for aqueous MDEA and hybrid solutions at different temperatures.

Regeneration of the solutions showed the role of the physical solvent (sulfolane) that yields

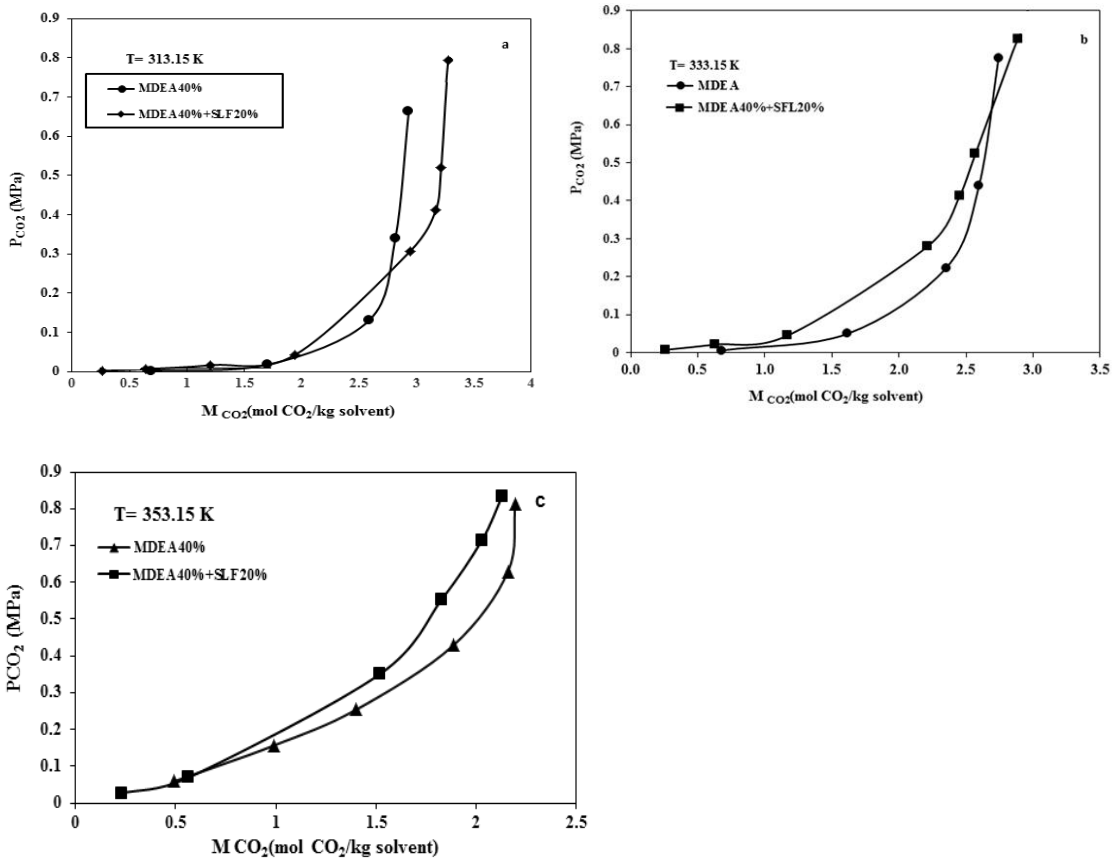

Fig. 9. The molality of CO_2 in different solutions at 313.15, 333.15, and 353.15 K.

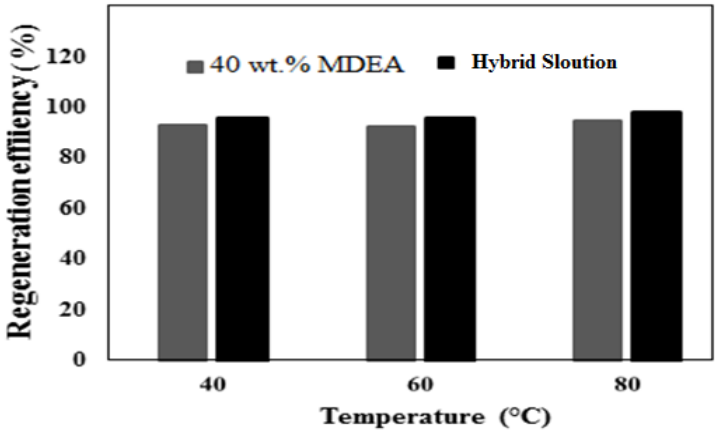

Fig. 10. Regeneration efficiency for 40wt.% MDEA and hybrid solutions at different temperatures

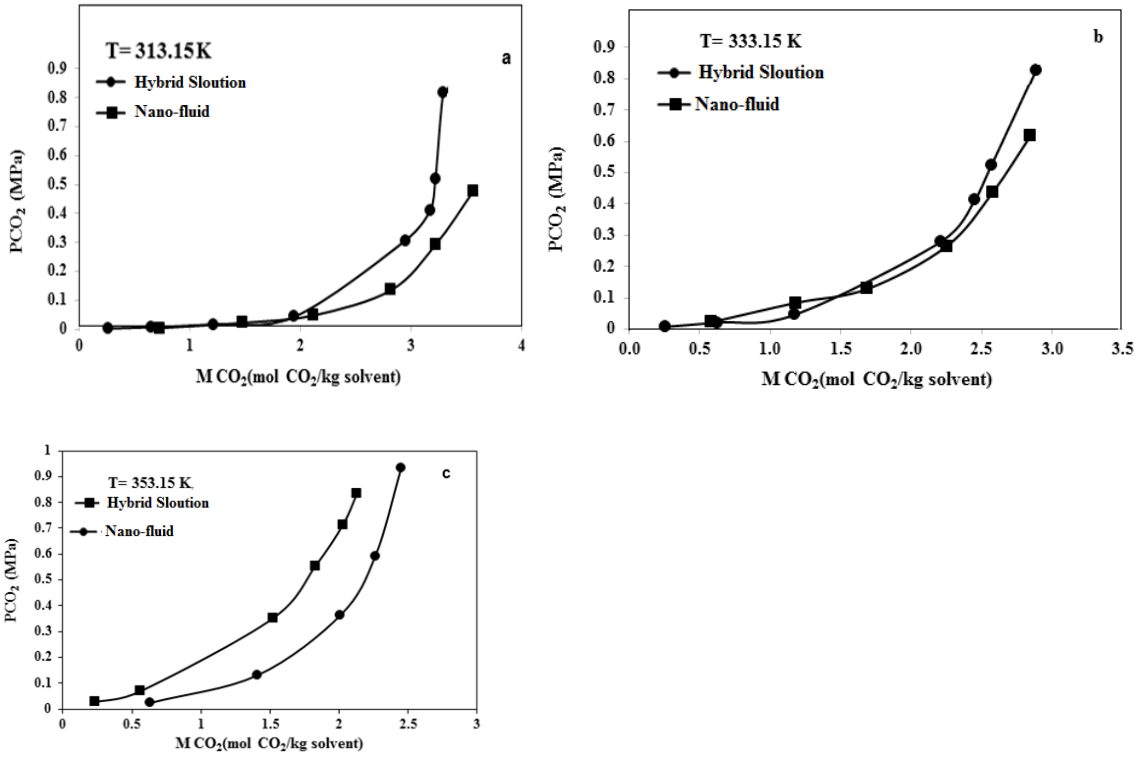

Fig. 11. The molality of CO_2 in hybrid solution and the nano-fluid at 313.15, 333.15, and 353.15K.

higher regeneration efficiencies for the hybrid solutions Figure 10. The regeneration efficiency for the composite MDEA solution after 5 cycles was 94.56% while that for the aqueous MDEA solution was 98.23%. To ensure a homogeneous dispersion of the nanoparticles in the hybrid solvent and to minimize their agglomeration, ultrasonic equipment is commonly used to disperse particles and reduce the agglomeration of nanoparticles. It has been shown that, the total regeneration energy (E_{regen}) consists of three components: reaction heat (Q_{rxn}), sensible heat (Q_{sens}), and latent heat (Q_{latent}). When the physical solvent sulfolane is used to replace part of the water in the solvent, caused a decrease in the sensible and latent heat components, resulted in a reduction in the total regeneration energy (Wang et al., 2019). Since, the regeneration temperatures for both aqueous and hybrid solutions were the same, the remained CO_2 after desorption in the hybrid solution is lower than that for the aqueous solution, and thus the

absorption capacity of the regenerated hybrid solution is higher than that of the regenerated aqueous solution.

Absorption tests were performed using the hybrid solution mixed with the 0.1wt.% MIL-101-NH_2(Cr) nano-particles (nano-fluid). Figure 11(a-c) shows the molality of CO_2 in the hybrid solution and the nano-fluid at 313.15, 333.15, and 353.15 K. As shown, addition of MIL-101-NH_2(Cr) nano-particles to the hybrid solution increases the molality of CO_2, approaching that of the aqueous solution (40wt.% MDEA) at low pressures and to some extent higher than that of the aqueous MDEA at high pressures (Figure 11). The molality of CO_2 for the nano-fluid reached 3.55 $mol.kg^{-1}$ that is about 17.1% higher than that of the aqueous MDEA at the temperature of 313.15k Compare figures 9(a) and 12(a).

As shown, MIL-101-NH_2(Cr) sample enhanced absorption capacity. Both the porous surface and the amine functional groups in the sample contribute to the increased overall CO_2 adsorption capacity in MIL-101 -NH_2(Cr). From an electrostatic perspective, the amino nitrogen's partial negative charge can interact favorably with CO_2 partial positive charge on carbon. In addition, the oxygen in CO_2 can create hydrogen bonds with the hydrogen in -NH_2. Because functional amine groups facilitate CO_2 uptake even when water is present, these characteristics can improve CO_2 uptake.

Based on the experimental results, MIL-101-NH2(Cr) exhibited a high specific surface area of 339.58 (BET), a total pore volume of 0.41 (BJH), and an average pore diameter of 3.64 nm. These characteristics indicate a well-developed porous structure and a strong capacity for gas adsorption.

Also, nanoparticles increase the mass transfer rate and provide larger surface area for CO_2 absorption (San Ho et al., 2021). Since the greatest resistance to mass transfer occurs at the phase interface, the effects of bubble breaking, hydrodynamics, and the shuttle mechanism can be considered, even though a precise mechanism has not yet been established. Nanoparticles are dispersed in the solution, and the micro bubbles that rise from the bottom of the solution collide with each other. The bubbles that flow in the solution provide kinetic energy to the particles and cause them to move more actively. The bubbles broke and change shape because of the collision with the particles on the gas-liquid interface. Therefore, the gas-liquid contact surface increases which in turn increases the absorption rate (Lee et al., 2016). A different effect that changes the mass transfer is the hydrodynamic effect in the double boundary layer. This effect makes the effective penetration layer smaller when nanoparticles hit each other and make turbulence at the gas-liquid interface. The changes in the gas-liquid interface also increase the mass transfer. In this case, mass permeation and the interface of two gas and liquid phases play the most important role (Fang et al., 2017).

Another proposed mechanism is shuttle mechanism. In this mechanism, first gas molecules are adsorbed on nanoparticle surfaces at the interface of two phases by the gas solubility shuttle

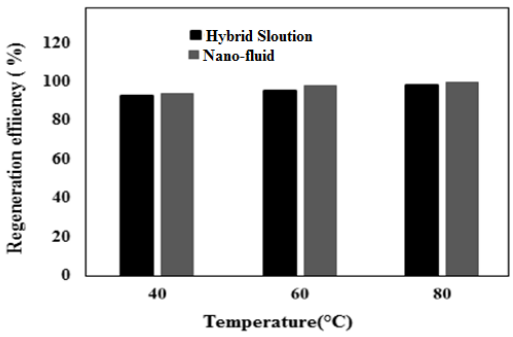

Fig. 12. Regeneration efficiency for hybrid solution and the nano-fluid.

Table 3. Summary of Experimental Tests

Test Type	Objective	Method / Standard Used
Hydrothermal synthesis of MIL-101-NH_2(Cr)	To synthesize nanostructured MOF particles with high surface area and porosity for enhanced CO_2 capture	Hydrothermal technique using $Cr(NO_3)_3 \cdot 9H_2O$ and 2-aminoterephthalic acid at 150 °C for 12 h in stainless steel autoclave
Zeta potential analysis	To evaluate the colloidal stability of nanofluid and ensure uniform nanoparticle dispersion	Malvern Zetasizer; stable suspensions identified by
Fourier Transform Infrared Spectroscopy (FTIR)	To identify chemical bonds, functional groups, and confirm amine functionalization of MIL-101-NH_2(Cr)	Bruker ISS-88 FTIR Spectrometer (ASTM E168 / E1252)
X-Ray Diffraction (XRD)	To determine crystal structure and phase purity of MIL-101-NH_2(Cr)	Bruker D8 ADVANCE XRD, Cu Kα radiation (ASTM D3906)
Scanning Electron Microscopy (SEM) & Transmission Electron Microscopy (TEM)	To study particle morphology, size distribution, and surface structure of synthesized nanoparticles	SEM: FEI Quanta 2000; TEM: Philips EM208 (ASTM E1508)
Brunauer–Emmett–Teller (BET) Analysis	To determine surface area, pore volume, and pore diameter of MIL-101-NH_2(Cr)	N_2 adsorption–desorption at 77 K using BELSORP Mini II (ISO 9277:2010)
Thermogravimetric Analysis (TGA)	To assess the thermal stability of MIL-101-NH_2(Cr) and its regeneration temperature limit	Perkin-Elmer TGA; heating from 25 °C–600 °C under N_2 atmosphere (ASTM E1131)
CO_2 Absorption Test	To measure CO_2 absorption capacity under varying pressure (0.1–5 MPa) and temperature (313–353 K)	High-pressure equilibrium reactor setup; solubility calculations per NIST standards
Regeneration Efficiency Test	To evaluate the solvent recyclability after multiple absorption–desorption cycles	Thermal desorption at 80 °C; efficiency calculated as ratio of recovered to fresh absorption capacity
Validation Test	To confirm accuracy of the experimental setup by comparing CO_2 solubility data with literature	Reference: 40 wt.% MDEA aqueous solution data from Vahidi et al. (2016) and Maleki et al. (2018)

mechanism. In the next steps, the gas solubility is enhanced when the nanoparticles enter the solution and absorb the adsorbed gas (Linek et al., 2008). The regeneration efficiency studied for hybrid solution and the nano-fluid. Figure 12 shows the regeneration efficiencies at different temperatures. As shown, addition of nanoparticles increased the regeneration efficiencies. This figure reveals that, the amount of CO_2 remaining in the nanofluid after the desorption process is less than that of the hybrid solution without nanoparticles which in turn direct to easier desorption process.

Consequently, simultaneous use of MIL-101-NH_2(Cr) nanoparticles and sulfolane as a physical solvent not only enhanced the molality of CO_2 and absorption capacity, but also, significantly improved the regeneration efficiency. A summary of the experimental tests is presented in Table 3.

CONCLUSIONS

This study examined CO_2 absorption and desorption using three solvent systems: aqueous MDEA, an MDEA–sulfolane hybrid, and a nano-hybrid solution containing MIL-101-NH_2(Cr). The results showed that sulfolane improved CO_2 absorption under high-pressure conditions and improved regeneration efficiency. The incorporation of MIL-101-NH_2(Cr) nanoparticles further increased absorption capacity by 17.1% and improved regeneration. The proposed hybrid system combines the chemical reactivity of MDEA, the physical absorption capacity of sulfolane, and the nanostructured advantages of MIL-101-NH_2(Cr), offering an efficient, stable, and low-cost approach for CO_2 capture. Future work should focus on scaling up the hybrid MDEA–sulfolane–MIL-101-NH_2(Cr) system for pilot-scale and industrial applications

to evaluate long-term stability, nanoparticle dispersion, and solvent recyclability under realistic operating conditions. Further studies could investigate optimization of nanoparticle concentration to balance performance and cost.

This study contributes to energy sustainability by developing an energy-efficient solvent that reduces regeneration heat duty and minimizes process energy consumption. Environmentally, it supports carbon emission reduction goals by enhancing CO_2 capture efficiency, thereby mitigating the impact of greenhouse gases from fossil fuel processing and combustion. Economically, the system's use of low-cost, regenerable materials (sulfolane and MIL-101-NH_2(Cr)) reduces operational expenses, extends solvent life, and enhances process profitability. Overall, this research advances the development of cost-effective and sustainable CO_2 capture technologies that align with global energy transition and environmental protection objectives.

NOMENCLATURES AND ABBREVIATIONS

MDEA	N-Methyldiethanolamine
DEA	Diethanolamine
DMF	Dimethylformamide
MOF	Metal Organic Framework
V_{gc}	Volumes of the gas container
ρ_i	Initial molar density of CO2
ρ_f	Final molar density of CO2
n_{co2}^{l}	Amount of CO2 in the liquid phase
n_{co2}^{g}	Moles of CO2 in the gas phase
Vg	Volume of gas-phase
ρ_{co2}^{g}	Molar density of CO2 in the gas phase
$V_{unloaded\ solvent}$	Volume of the unloaded solvent
M_{CO_2}	Molality
$w_{unloaded\ solvent}$	Fresh nanofluid solvent
α_{CO_2}	CO2 absorption on loading
TK	Temperature
$u(p_k)$	Uncertainty of the pressure sensors
Q_{latent}	Iatent heat
Q_{rxn}	Reaction heat
Q_{sens}	Sensible heat
E_{regen}	Total regeneration energy

Diagram of the steps for performing experimental analysis

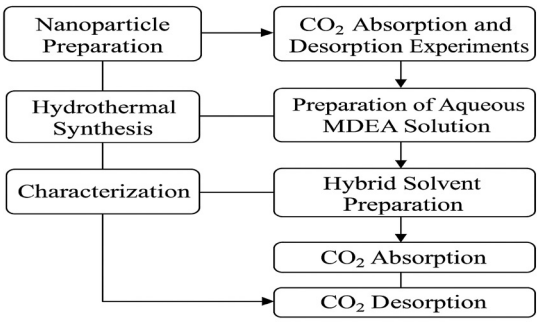

GRANT SUPPORT DETAILS

The present research did not receive any financial support.

CONFLICT OF INTEREST

The authors declare that there is not any conflict of interests regarding the publication of this manuscript. In addition, the ethical issues, including plagiarism, informed consent, misconduct, data fabrication and/ or falsification, double publication and/or submission, and redundancy has been completely observed by the authors.

LIFE SCIENCE REPORTING

No life science threat was practiced in this research.

REFERENCES

Bahadori, M. K., Golhosseini, R., Shokouhi, M., & Zoghi, A. T. (2024). Mixing γ-Al2O₃, silica-ZIF-8, and activated carbon nanoparticles in aqueous N-methyldiethanolamine + sulfolane as a nanofluid for application on CO_2 absorption. *Journal of CO_2 Utilization, 79*, 102650.

Belmabkhout, Y., Guillerm, V., & Eddaoudi, M. (2016). Low-concentration CO_2 capture using physical adsorbents: Are metal–organic frameworks becoming the new benchmark materials? *Chemical Engineering Journal, 296*, 386–397.

Borhani, T. N., Oko, E., & Wang, M. (2018). Process modelling and analysis of intensified CO_2 capture using monoethanolamine (MEA) in a rotating packed bed absorber. *Journal of Cleaner Production, 204*, 1124–1142.

Borhani, T. N., & Wang, M. (2019). Role of solvents in CO_2 capture processes: A review of selection and design methods. *Renewable and Sustainable Energy Reviews, 114*, 109299.

Carretero-Cerdán, A., Carrasco, S., Sanz-Marco, A., Jaworski, A., & Martin-Matute, B. (2023). One-step microwave-assisted synthesis of amino-functionalized chromium (III) terephthalate MIL-101-NH_2(Cr). *Materials Today Chemistry, 31*, 101618.

Fang, L., Liu, H., Bian, Y., Liu, Y., & Yang, Y. (2017). Experimental study on enhancement of bubble absorption of gaseous CO_2 with nanofluids in ammonia. *Journal of Harbin Institute of Technology, 24*(2), 80–86.

Ghadimi, A., Saidur, R., & Metselaar, H. (2011). A review of nanofluid stability properties and characterization in stationary conditions. *International Journal of Heat and Mass Transfer, 54*(17–18), 4051–4068.

Ghasemi, M. H., Irani, V., & Tavasoli, A. (2020). Amino functionalized ZIF-90@GO/MDEA nanofluid: A new class of multi-hybrid systems to enhance the performance of amine solutions in CO_2 absorption. *Journal of Natural Gas Science and Engineering, 74*, 103110.

Gouedard, C., Picq, D., Launay, F., & Carrette, P. L. (2012). Amine degradation in CO_2 capture. I. A review. *International Journal of Greenhouse Gas Control, 10*, 244–270.

Haghtalab, A., & Shirazizadeh, H. A. (2019). An electrolyte segmental Wilson–nonrandom excess Gibbs energy model and measurement of carbon dioxide solubility in sulfolane + water and N-methyldiethanolamine + sulfolane + water systems. *Journal of Molecular Liquids, 296*, 111786.

Irani, V., Tavasoli, A., & Vahidi, M. (2018). Preparation of amine functionalized reduced graphene oxide/methyl diethanolamine nanofluid and its application for improving the CO_2 and H_2S absorption. *Journal of Colloid and Interface Science, 527*, 57–67.

Irani, V., Khosh, A. G., & Tavasoli, A. (2020). Polyethyleneimine (PEI) functionalized metal oxide nanoparticles recovered from the catalytic converters of spent automotive exhaust systems and application for CO_2 adsorption. *Frontiers in Energy Research, 8*, 196.

Kidnay, A. J., Parrish, W. R., & McCartney, D. G. (2019). *Fundamentals of natural gas processing*. CRC Press.

Lee, J. W., Pineda, I. T., Lee, J. H., & Kang, Y. T. (2016). Combined CO_2 absorption/regeneration performance enhancement by using nanoabsorbents. *Applied Energy, 178*, 164–176.

Liang, Z., Fu, K., Idem, R., & Tontiwachwuthikul, P. (2016). Review on current advances, future challenges and consideration issues for post-combustion CO_2 capture using amine-based absorbents. *Chinese Journal of Chemical Engineering, 24*(2), 278–288.

Linek, V., Kordač, M., & Soni, M. (2008). Mechanism of gas absorption enhancement in the presence of fine solid particles in mechanically agitated gas–liquid dispersion: Effect of molecular diffusivity. *Chemical Engineering Science, 63*(21), 5120–5128.

Luo, W., Guo, D., Zheng, J., Gao, S., & Chen, J. (2016). CO_2 absorption using biphasic solvent: Blends of diethylenetriamine, sulfolane, and water. *International Journal of Greenhouse Gas Control, 53*, 141–148.

Maleki, A., Irani, V., Tavasoli, A., & Vahidi, M. (2018). Enhancement of CO_2 solubility in a mixture of 40 wt% aqueous N-methyldiethanolamine solution and diethylenetriamine functionalized graphene oxide. *Journal of Natural Gas Science and Engineering, 55*, 219–234.

Mumford, K. A., Wu, Y., Smith, K. H., & Stevens, G. W. (2015). Review of solvent based carbon-dioxide capture technologies. *Frontiers of Chemical Science and Engineering, 9*, 125–141.

Nozaeim, A. A., Mortaheb, H. R., Tavasoli, A., & Mafi, M. (2022). CO_2 absorption/desorption rates in aqueous DEEA/MDEA and sulfolane-contained hybrid solutions: Effects of physical properties and reaction rate. *Environmental Science and Pollution Research, 29*(25), 38633–38644.

Piscopo, C. G., & Loebbecke, S. (2020). Strategies to enhance carbon dioxide capture in metal–organic frameworks. *ChemPlusChem, 85*(3), 538–547.

San Ho, P., Chong, K. C., Lai, S. O., Mah, S. K., Lee, S. S., Lu, S. Y. (2021). Synthesis of MIL-101 (Cr) metal organic framework by green synthesis for CO_2 gas adsorption. In *IOP Conference Series: Earth and Environmental Science*. IOP Publishing.

Tian, N., Jia, Q., Su, H., Zhi, Y., Ma, A., Wu, J., & Shan, S. (2016). The synthesis of mesostructured NH_2-MIL-101 (Cr) and kinetic and thermodynamic study in tetracycline aqueous solutions. *Journal of Porous Materials, 23*, 1269–1278.

Vahidi, M., Tavasoli, A., & Rashidi, A. M. (2016). Preparation of amine functionalized UiO-66, mixing with aqueous N-methyldiethanolamine and application on CO_2 solubility. *Journal of Natural Gas Science and Engineering, 28*, 651–659.

Wang, L., Liu, S., Wang, R., Li, Q., & Zhang, S. (2019). Regulating phase separation behavior of a DEEA–TETA biphasic solvent using sulfolane for energy-saving CO_2 capture. *Environmental Science & Technology, 53*(21), 12873–12881.

Xu, A., Chen, Z., Jin, L., Chu, B., Lu, J., He, X. (2021). Quaternary ammonium salt functionalized MIL-101-NH_2 (Cr) as a bifunctional catalyst for the cycloaddition of CO_2 with epoxides to produce cyclic carbonates. *Applied Catalysis A: General, 624*, 118307.

Yih, S. M., & Sun, C. C. (1987). Simultaneous absorption of hydrogen sulfide and carbon dioxide into di-isopropanolamine solution. *The Canadian Journal of Chemical Engineering, 65*(4), 581–585.

Zheng, C., Tan, J., Wang, Y. J., & Luo, G. S. (2013). CO_2 solubility in a mixture absorption system of 2-amino-2-methyl-1-propanol with ethylene glycol. *Industrial & Engineering Chemistry Research, 52*(34), 12247–12252.